Constraining the Imaginary Refractive Index of Brown Carbon via an Observation-Informed Inversion Framework

Hye-eun Cho[1], Minjoong J. Kim[2], Seohee H. Yang[3], Yongjoo Choi[4], Minseo Lee[4], and Seungun Lee[5]

[1]Department of Environmental and Energy Engineering, College of Engineering, Myongji University, Yongin, Republic of Korea (fldywndghk@naver.com)
[2]Department of Environmental Systems Engineering, College of Engineering, Myongji University, Yongin, Republic of Korea (minjoongkim@mju.ac.kr)
[3]Research Institute of Basic Sciences, Seoul National University, Seoul, Republic of Korea (seoheey0428@snu.ac.kr)
[4]Department of Environmental Science, Hankuk University of Foreign Studies, Yongin, Republic of Korea (choingjoo@hufs.ac.kr, naminseo03@hufs.ac.kr)
[5]Department of Earth and Environmental Sciences, Seoul National University, Seoul, Republic of Korea (hb3099@hotmail.com)

EGU26 GENERAL ASSEMBLY

Hall X5 | X5.39

EGU26-6214

INTRODUCTION

- Global anthropogenic aerosol optical depth has changed little since the 1980s, but the fraction of absorbing aerosols has nearly doubled (Williams et al., 2022).
- Among absorbing aerosols, mineral dust, black carbon (BC), and brown carbon (BrC) absorb solar radiation, alter aerosol single-scattering albedo, and influence atmospheric radiative forcing (Tuccella et al., 2020).
- BrC, the light-absorbing fraction of organic aerosol, exhibits stronger absorption at shorter wavelengths and can exceed BC absorption in the ultraviolet region (Kirchstetter et al., 2012; Du et al., 2022; Yan et al., 2025).
- Accurate estimates of aerosol optical properties and radiative effects require wavelength-dependent complex refractive indices.
- However, observational constraints on the refractive index of BrC remain limited, with previous studies restricted to specific regions or narrow wavelength ranges, leading to large uncertainties in BrC absorption and its radiative forcing effects (Shamjad et al., 2016; Womack et al., 2021; Deng et al., 2022).
- Therefore, this study constrains the wavelength-dependent imaginary refractive index of BrC over South Korea using an observation-informed inversion framework based on the observed Absorption Ångström Exponent (AAE), and evaluates its impacts on aerosol optical properties and shortwave radiative forcing.

DATA

1) Observation

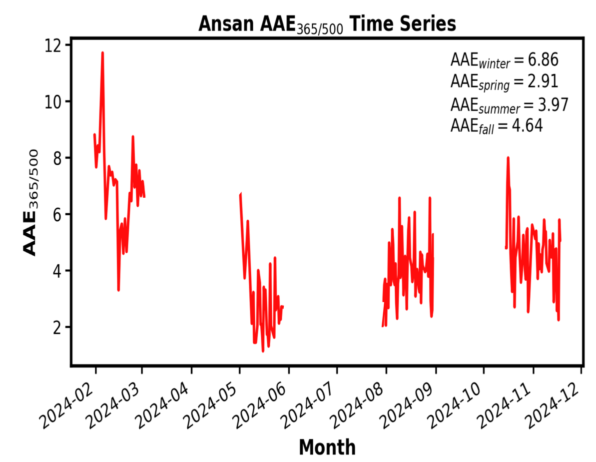

	Feb	May	Aug	Oct
Abs_{365} (Mm^{-1})	1.97	2.18	1.40	2.65
Abs_{500} (Mm^{-1})	0.16	0.89	0.34	0.47
$AAE_{365/500}$	6.86	2.91	3.97	4.64
MAE_{440} ($m^2\ g^{-1}$)	0.17	0.96	0.43	0.42

- The observational data used in this study were collected in Ansan, South Korea (37.320°N, 126.828°E) during representative seasonal periods in February, May, August, and October 2024.
- $PM_{2.5}$ samples were extracted using water as a solvent, and the absorption coefficient (Abs) was measured using a UV–Vis spectrometer to derive the aerosol absorption Ångström exponent (AAE).
- The derived AAE values were highest in winter, followed by autumn, summer, and spring.

2) Modeling Framework for Aerosol Concentrations

- A coupled GRIMs-CCM and WRF-GC modeling system was used to estimate aerosol concentrations for 2020–2050.
- Because both models share the GEOS-Chem chemistry module, global outputs were dynamically downscaled to regional-scale concentrations, with analysis focused on 2020–2025.
- To reduce the underestimation of surface aerosols and gaseous species, concentrations over South Korea were bias-corrected using observations from 580 AirKorea AQMS sites, improving PM_{10} NMB from 54% to 31.3% and $PM_{2.5}$ NMB from 69.7% to 32%.
- To mitigate overestimation in the middle atmosphere, the vertical aerosol distribution was corrected using species-resolved profiles from the 2024 CAMS reanalysis, improving AOD_{550} NMB from 458% to −84.5%.

	GRIMs-CCM	WRF-GC
Domain	0–360°E, 90°S–90°N	112.78–134.25°E, 29.12–45.04°N
Spatial resolution	1.825° × 1.825° 47 vertical layers	45 km × 45 km 29 vertical layers
• Global: Sea Boundary Conditions • Regional: Meteorological and Chemical initial/boundary condition	CMIP6 (8-model ensemble) :Sea Surface Temperature, Snow Depth, Sea Ice Concentration	GRIMs-CCM SSP5-8.5 global output
Anthropogenic Emission	Input4mips SSP1-2.6, SSP5-8.5	South Korea 2030 NDC scenario

METHODS

1) Estimation of BrC Concentration Using the BrC/OC Ratio

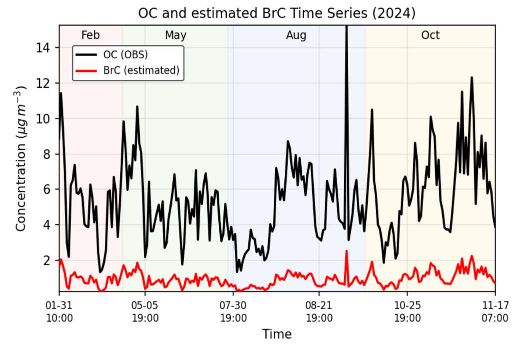

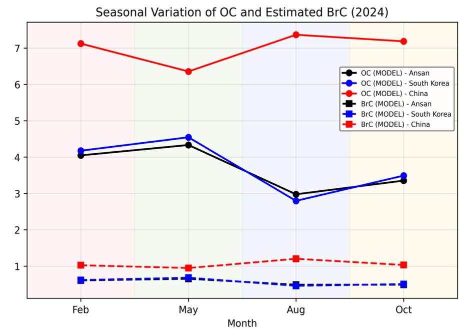

Month	OC ($\mu g/m^3$)				BrC ($\mu g/m^3$)			
	OBS	MODEL			OBS	MODEL		
		Ansan	South Korea	China		Ansan	South Korea	China
Feb	5.08	4.05	4.17	7.12	0.91	0.61	0.62	1.02
May	5.16	4.33	4.54	6.36	0.9	0.65	0.68	0.95
Aug	4.94	2.98	2.80	7.37	0.82	0.49	0.46	1.20
Oct	5.38	3.35	3.49	7.19	0.98	0.49	0.50	1.03

- OC was partitioned into WSOC (OCPI) and WIOC (OCPO), and seasonal fractions from Seoul observations (Lee et al., 2020) were applied to estimate BrC.
- BrC fractions based on highly condensed aromatics (AI ≥ 0.67) yielded BrC/OC ≈ 17–18% (Zhang et al., 2024; Mo et al., 2024), within the reported range (Xiong et al., 2022).
- Modeled OC and BrC were 2.98–4.33 and 0.49–0.65 μg m^{-3} (Ansan), 2.80–4.54 and 0.46–0.68 μg m^{-3} (South Korea), and 6.36–7.37 and 0.95–1.20 μg m^{-3} (China).
- Although OC was underestimated, simulated BrC remained within the global range (0.005–10.54 μg m^{-3}; Jiang et al., 2026), likely due to the strict definition of BrC (highly condensed aromatics only).

2) BC/OC Ratio Diagnostic

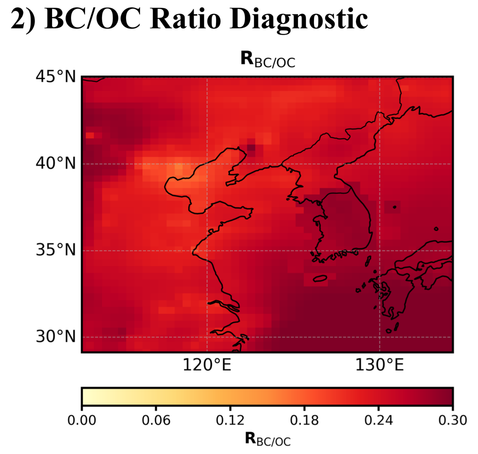

- The BC-to-OC mass ratio ($R_{BC/OC}$) was used to interpret regional BrC responses in the 2020–2025 mean.
- High $R_{BC/OC}$ indicates BC-rich conditions enhancing absorption, while low $R_{BC/OC}$ indicates OC-rich conditions sensitive to optical assumptions.
- his metric explains spatial variability in AAOD, AOD, and SSA.

3) Optical Property Calculations

$$m = n - ik \quad (1)$$

$$AAE = -\frac{\ln(AAOD_{365}/AAOD_{500})}{\ln(365/500)} \quad (2)$$

$$AAOD = k\lambda^{-AAE} \quad (3)$$

$$AAOD = AOD \cdot (1 - SSA) \quad (4)$$

$$AOD = \sigma_e \cdot \Delta z \quad (5)$$

$$SSA = \frac{\sigma_s}{\sigma_s + \sigma_a} = \frac{\sigma_s}{\sigma_e} \quad (6)$$

- The refractive index describes light speed and absorption (Eq. 1), with k representing BrC absorption.
- Seasonal k_{440} values were derived to estimate BrC refractive indices over 250–40000 nm.
- To reduce uncertainties from relative humidity (RH)-dependent bleaching during aging, which is stronger under high-RH conditions (Duan et al., 2025), k values were calculated at RH = 50%.
- Optical properties were computed using Eqs. 2–6.

4) Inversion of BrC Imaginary Refractive Index (k)

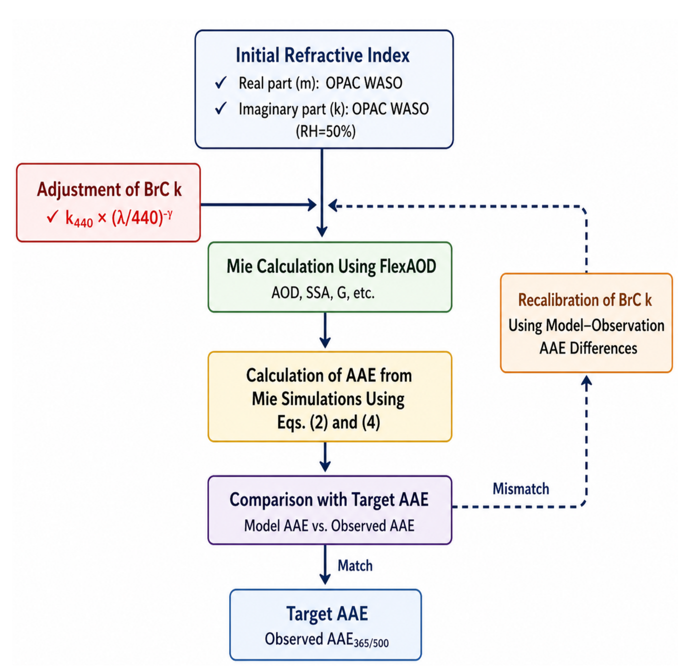

Species	Density ($g\ cm^{-3}$)	Radius (μm)	Refractive index
OC	1.8	0.063	OPAC WASO (OC k ≈ 0 ;BrC absorption included)
BC	1.8	0.02	OPAC SOOT
BrC	1.8	0.063	n: OPAC WASO (RH = 50%) k: This study (RH = 50%)

$$MAE_{\lambda}^{obs}[m^2/g] = \frac{\overline{Abs_{\lambda}}}{\overline{M}} \quad (7)$$

$$MAE_{\lambda}^{model}[m^2/g] = \frac{AAOD}{BrC\ [g/m^2]} \quad (8)$$

$$k = k_{440} \cdot \left(\frac{\lambda}{440}\right)^{-\gamma} \quad (9)$$

- k_{440} was determined by matching the observation-based mass absorption efficiency (MAE_{λ}^{obs}) with the model-based mass absorption efficiency (MAE_{λ}^{model}).
- MAE_{λ}^{obs} was calculated from observed BrC mass concentration and absorption coefficients, while MAE_{λ}^{model} was derived from BrC mass loading per unit area and AAOD (Eqs. 7–8).
- Wavelength-dependent k was estimated assuming a power-law relationship between absorption optical depth (AAOD) and wavelength (Eq. 9).
- Since k is proportional to AAOD, wavelength-dependent k was optimized by varying γ in repeated Mie calculations until the target AAE was reproduced.
- Radiative forcing was then calculated using the Rapid Radiative Transfer Model – Short Wave (RRTMG-SW).

RESULTS

1) Optical Absorption Properties of BrC

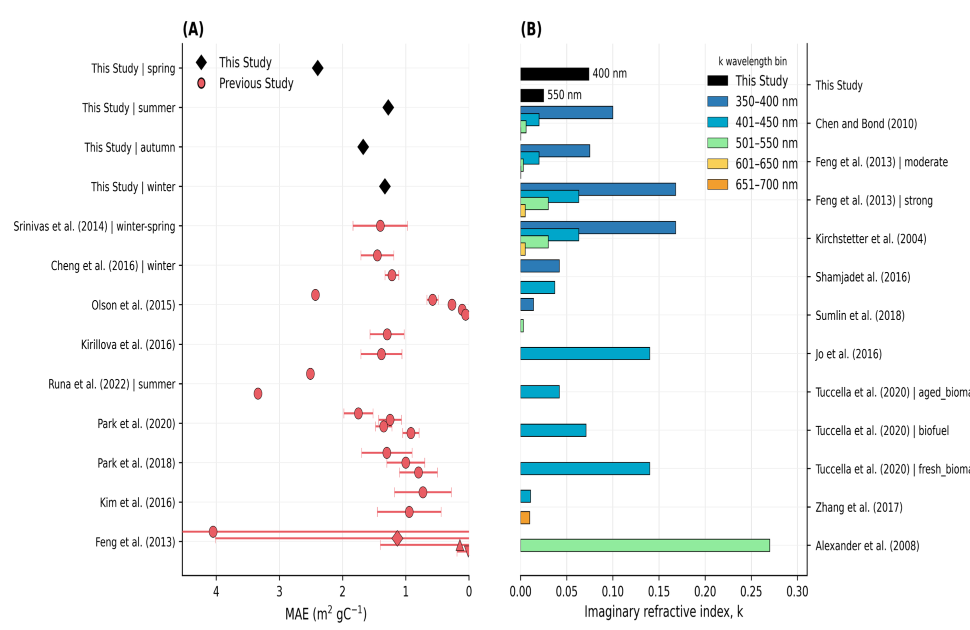

- MAE values reported in $m^2\ g^{-1}$ were converted to $m^2\ gC^{-1}$ using OM/OC = 1.8.
- Both the derived MAE_{440} and k values were within the ranges reported in previous studies.
- Although the estimated MAE_{440} fell within the reported range, it was relatively lower than values observed in China and in biomass-burning influenced regions.
- This likely reflects the emission characteristics of Ansan, where industrial, traffic, and urban sources dominate, while contributions from biomass burning are relatively limited.

Month	MAE_{440} ($m^2\ gC^{-1}$)	MAE_{440} ($m^2\ g^{-1}$)	k_{440}	$AAE_{365/500}^{obs}$	$AAE_{365/500}^{model}$	k_{400}	k_{550}
Feb	1.33	0.74	0.042	6.86	6.86	0.075	0.010
May	2.40	1.33	0.078	2.91	2.91	0.096	0.048
Aug	1.28	0.71	0.032	3.97	3.967	0.042	0.017
Oct	1.67	0.93	0.056	4.64	4.64	0.082	0.023

2) Validation of Aerosol Absorption Properties

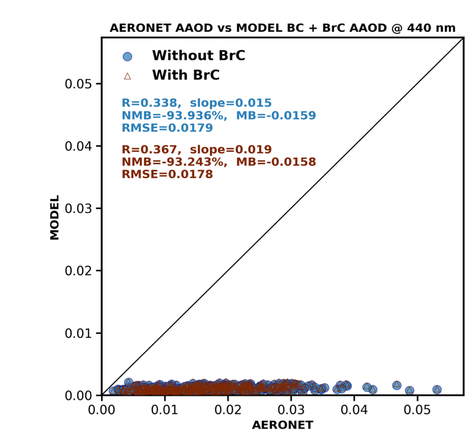

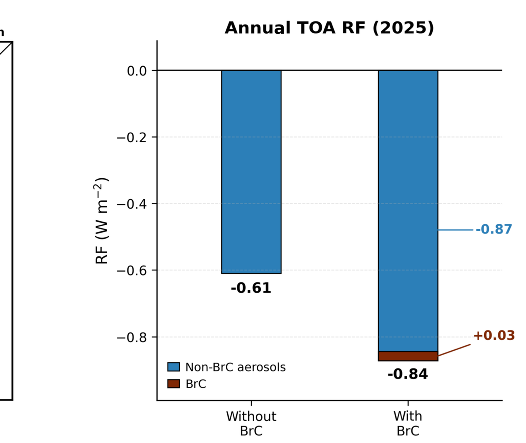

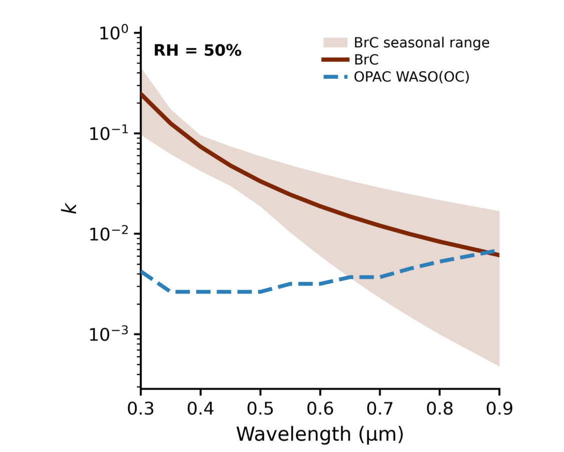

- The derived BrC k was used to evaluate AAOD against AERONET data, showing slight performance improvement when BrC was included (R: 0.338 → 0.367, with reduced NMB and RMSE).
- Radiative forcing (RF) in the With BrC case (~0.03 W m^{-2}) was slightly lower than previous estimates (Jo et al., 2016: 0.038 W m^{-2}; Park et al., 2010: 0.05 W m^{-2}), likely due to applying WSOC-based absorption properties to WIOC.
- Despite BrC being an absorbing aerosol, RF became more negative, indicating enhanced scattering.
- This behavior is attributed to the assumption of negligible OC absorption when BrC is introduced.
- The derived BrC k showed weak visible-light absorption, whereas OPAC OC exhibited stronger absorption toward longer visible wavelengths.
- This contrast likely explains the reduction in AAOD and the more negative radiative forcing when OC absorption was replaced by BrC.
- Thus, accurate treatment of visible-wavelength OC absorption, including the separation of BrC and non-BrC OC, is essential for reliable aerosol radiative forcing estimates.

3) Impacts of BrC on Aerosol Optical Properties

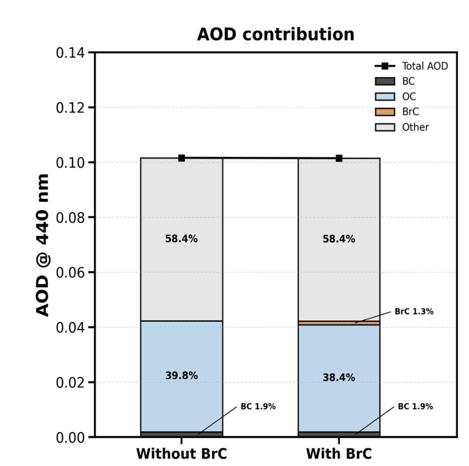

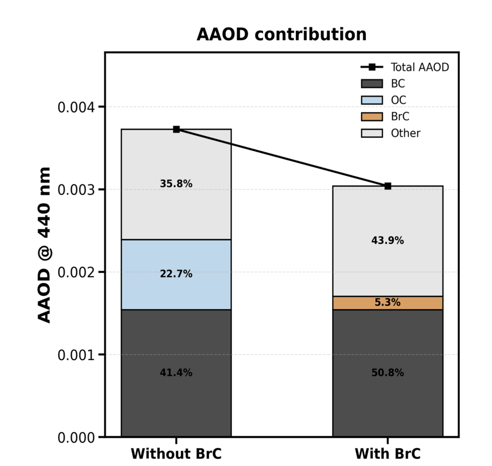

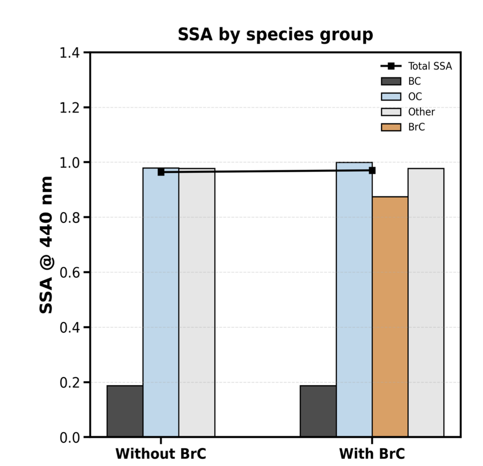

	species	AOD@440 nm	AAOD @440nm	SSA @440nm
Without BrC	BC	0.0019	0.0015	0.1876
	OC	0.0404	0.0008	0.9787
	Others	0.0529	0.0007	0.9872
	Bulk Total	0.1016	0.0037	0.940
With BrC	BC	0.0019	0.0015	0.1876
	BRC	0.0013	0.0002	0.8632
	Others	0.0578	0.0007	0.8587
	OC	0.0390	0.000	1.0000
	Bulk Total	0.1015	0.0030	0.9704

- Consistent with the contrasting spectral absorption behavior, AAOD decreases (0.0037 → 0.0030) when BrC is included.
- This indicates that replacing OC absorption with BrC leads to a net reduction in aerosol absorption.
- In particular, BrC absorption (AAOD ≈ 0.0002) is smaller than the original OC absorption (AAOD ≈ 0.0008), demonstrating that BrC does not fully compensate for OC absorption.
- This result is consistent with the wavelength-dependent behavior of BrC, whose absorption decreases toward longer wavelengths, leading to an overall reduction in bulk absorption.

4) Regional Responses to BrC Treatment (With BrC - Without BrC)

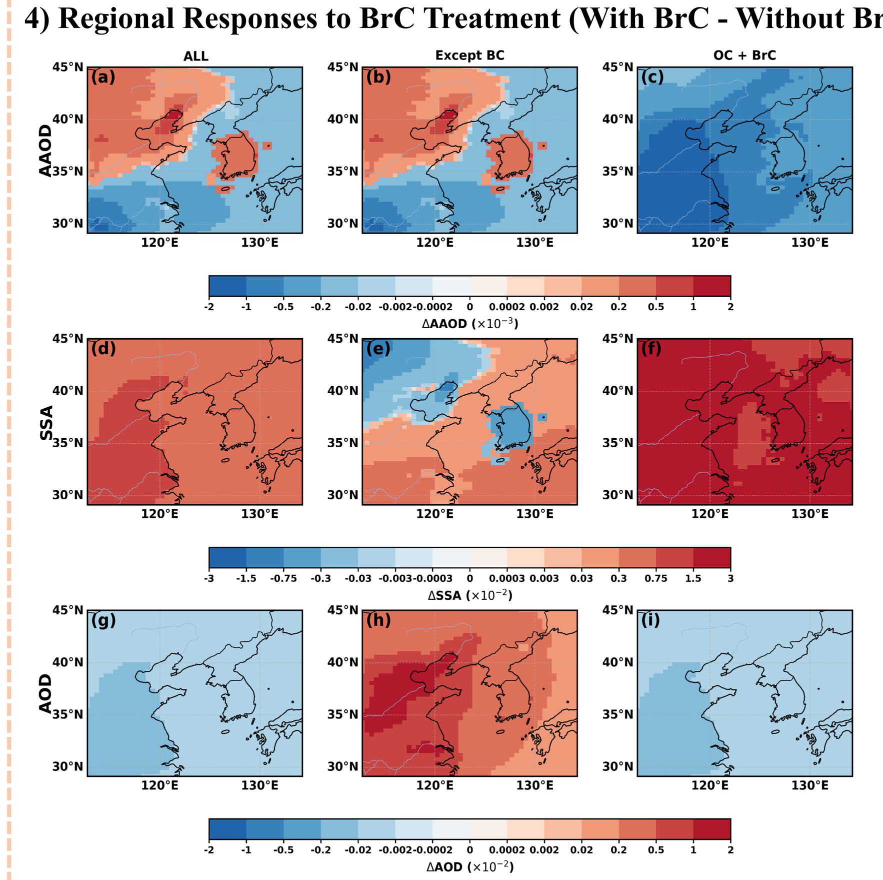

Spatial differences in AAOD, SSA, and AOD between With and Without BrC reflect the combined effects of $R_{BC/OC}$ and OC–BrC absorption characteristics.

1. ALL case

In regions with high $R_{BC/OC}$, BC absorption dominates, masking the effect of BrC.

In regions with low $R_{BC/OC}$, differences between OC and BrC absorption become evident, leading to decreased AAOD and increased SSA.

2. Except BC case

Similar patterns persist without BC, indicating that the changes are driven by OC–BrC absorption differences rather than BC.

Thus, OC–BrC absorption differences act as the physical driver of the response.

3. OC + BrC case

With OC absorption set to zero, AAOD represents BrC absorption alone.

AAOD is smaller and SSA is higher compared to the original OC case, indicating that BrC does not fully compensate for OC absorption.

CONCLUSIONS

- A practical observation-informed framework was developed to explicitly represent BrC in aerosol optical and radiative calculations over the South Korea.
- The wavelength-dependent imaginary refractive index (k, 250–40000 nm) was successfully constrained using observed seasonal MAE_{440} and AAE, with derived values consistent with previous studies.
- Including BrC slightly improved AAOD agreement with AERONET observations, increasing the correlation coefficient from 0.338 to 0.367 and reducing NMB and RMSE.
- However, AAOD decreased from 0.0037 to 0.0030 and SSA increased from 0.94 to 0.97, resulting in more negative radiative forcing (~0.03 W m^{-2}) despite the inclusion of an absorbing aerosol.
- This counterintuitive response arises from replacing OC absorption with BrC, whose absorption (AAOD ≈ 0.0002) is weaker than that of the original OC (AAOD ≈ 0.0008).
- Comparison with OPAC OC refractive indices revealed opposite spectral behavior, with BrC absorption decreasing and OC absorption increasing toward longer wavelengths.
- Regional analysis showed that BC/OC ratios control the visibility of BrC effects, while OC–BrC absorption differences act as the primary physical driver of aerosol optical responses.
- These results highlight significant uncertainties in OC absorption, particularly at longer wavelengths, and emphasize the need for improved constraints on both BrC and non-BrC OC in aerosol radiative forcing estimates.

FUTURE STUDIES

Future research will address three key limitations in the current framework.

1) Uncertainty in OC absorption (k) – Future work will better constrain OC refractive indices and their separation from BrC at longer wavelengths.

2) RH-dependent BrC absorption was not fully represented – Future work will explicitly include RH-driven bleaching and optical changes

3) BrC absorption may be underestimated for WIOC – Future studies will develop separate optical constraints for WIOC.

ACKNOWLEDGEMENT

This work was supported by the National Research Foundation of Korea(NRF) grant funded by the Korea government (MSIT) (No. RS-2025-16070879).